An atomistic description of the high-field degradation of dielectric polyethylene

Clive R. Bealing and R. Ramprasad
Department of Materials Science and Engineering, Institute of Materials Science, University of Connecticut, 97 North Eagleville Road, Storrs, Connecticut 06269-3136, USA

(Received 3 July 2013; accepted 23 September 2013; published online 6 November 2013)

A microscopic mechanism governing the initiating step in the high-field aging of crystalline polyethylene is proposed, based on density functional calculations and *ab initio* molecular dynamics simulations. It is assumed that electrons, holes, and excitons are present in the system. While the additional individual electrons or holes are not expected to lead to significant degradation, the presence of triplet excitons are concluded to be rather damaging. The electron and hole states of the exciton localize on a distorted region of polyethylene, significantly weakening nearby C–H bonds and facilitating C–H bond scission. The barrier to cleavage of the weakened C–H bonds is estimated and is comparable to the thermal energy, suggesting that this mechanism may be responsible for the degradation of polyethylene when placed under electrical stress, e.g., in high-voltage cables.
 [http://dx.doi.org/10.1063/1.4824386]

I. INTRODUCTION

Degradation of bulk polymeric dielectrics, such as polyethylene (PE), at high electric fields is critical in the dielectric failure of such materials.[1] The detailed chemistry by which such degradation takes place is not well understood, although in general polymer degradation relies on an initiating step in which primary bonds are broken and labile radical groups are created.[2] Data from electroluminescence (EL) and guarded needle experiments[1,3–6] indicate that rapid degradation is associated with positive and negative charge distributions passing through each other on a cyclic basis, i.e., on carrier recombination. Interestingly, Laurent *et al.*[4] have estimated a quantum efficiency for EL from carrier recombination in the range of just 10^{-6}, which suggests that the vast majority of the electron-hole pairs (excitons) generated by carrier recombination decay via nonradiative paths. The photons generated by EL are in the UV range (>3 eV) and can certainly cause bond cleavage; however, with such a low quantum efficiency for radiative relaxation, EL is unlikely to dominate polymer degradation. Bond cleavage may result from the creation of charge carriers sufficiently energetic to break bonds.[2] An alternative explanation is that bond scission results from nonradiative exciton recombination, which is consistent with the evidence from the EL and guarded needle measurements.

An understanding of the microscopic mechanism governing the creation of the chemical impurities associated with electrically stressed polymers is of fundamental as well as practical importance. The impurity groups formed as a result of the degradation generally lead to enhanced charge transport, which takes place between the associated localized "trap" states[1,2,7–9] which can cause a significant decline in dielectric properties.[2,10] This is problematic in applications that make use of polymeric insulation, such as high-voltage cables.

A number of reaction paths have been suggested[11,12] by which functional groups such as ketonic carbonyls – which are the groups most commonly observed after high field aging in PE – might be created. In general, these paths involve the reaction of the radicals produced during the initiating step with O_2. High field experiments carried out on degassed PE, PE saturated with N_2 or SF_6, and PE in air indicate that a lack of oxygen impedes degradation,[13] which suggests that oxygen plays an important role in the degradation process.

Previous first-principles studies have elucidated the interchain nature of the conduction states and intra-chain nature of the valence states in PE.[14,15] A density functional theory (DFT) investigation by Ceresoli *et al.* into self-trapping of excitons in bulk PE found that the exciton can self-trap on a distortion of a single chain, three C_2H_4 units in length.[16] A nonradiative exciton recombination path was not identified, and Ceresoli *et al.* concluded that excitons within the crystalline regions of PE were unlikely to damage the material. Ceresoli *et al.* also explored the possibility of damage to PE resulting from the nonradiative recombination of excitons trapped at various types of common impurities.[17] The behavior of the exciton was predicted to vary considerably depending on the nature of the impurity. While simple trapping of excitons was predicted at carbonyl defects, nonradiative exciton recombination was a possibility for excitons at vinyl groups and carboxyl groups within PE.

In this paper we use spin-polarized DFT calculations and *ab initio* molecular dynamics (MD) simulations to demonstrate that a nonradiative exciton recombination path *does* exist for pure PE. This recombination path, which proceeds by the breaking of a C–H bond, provides a microscopic mechanism governing the initiating step associated with aging in high field regions of PE.

Using DFT-based structural optimizations we studied the thermodynamics of C–H bond-breaking in PE for different electronic states. Electron occupations reflecting the presence of an additional electron in the conduction band, a hole in the valence band, and a triplet exciton were considered; bond-breaking was favored only for PE in the excitonic state.

During the course of that structural optimization the dissociated H subsequently abstracted a second H from the PE to form a H_2 dimer, leaving a pair of reactive –CH·– radicals along the main chains. The final structure, whose energy was 2.4 eV lower than that of the intact PE, was strongly thermodynamically favored. *Ab initio* MD simulations, in which a triplet exciton is injected into PE, reveal that the C–H bond cleavage occurs rapidly at room temperature, without an extended period of self-trapping. The exciton became self-trapped on a structural distortion characterized by a twist in the PE chains and a lengthening of the C–H bonds in the region in which the exciton is localized. Climbing image nudged elastic band (CINEB) DFT[18] calculations were used to estimate the energetic barrier for C–H bond cleavage and subsequent H abstraction from the distorted structure; the barrier to bond cleavage is comparable to the thermal energy at 300 K. H abstraction is barrierless when it takes place via a chain adjacent to that from which the cleavage took place; for cleavage and H abstraction from the same chain, barriers of 60 meV and 340 meV were estimated, where the final pair of –CH·– radicals were separated by a single $–CH_2–$ group or were directly adjacent, respectively. We considered the case of an exciton trapped on a pair of adjacent CH· defects and the possibility of radiative recombination leading to formation of a HC=CH vinyl defect in the PE. This path is hindered by the existence of the nonradiative recombination path identified by Ceresoli *et al.*, characterized by a $\sim 90^\circ$ distortion in the H–C–C–H dihedral. A MD simulation reveals that the system undergoes successive transitions between the distorted and undistorted conformations, thereby spending a small but significant amount of time in the excitonic state, which suggests that radiative recombination will eventually occur.

This article is organized as follows: In Sec. II the computational techniques employed are summarized. Section III A presents results on the thermodynamics of C–H bond cleavage for PE in different electronic states. In Sec. III B the results from an *ab initio* MD simulation in which a triplet exciton was injected into intact PE are discussed. In Sec. III C we explore the barriers to C–H bond cleavage and subsequent H abstraction using the CINEB method, and in Sec. III D dissociation and abstraction from the same chain are considered. In Sec. III E the possibility of radiative recombination for a pair of adjacent –CH·– radicals in PE is explored. Section IV presents a summary of this work and its conclusions.

II. COMPUTATIONAL METHODS

Unless stated otherwise, all DFT calculations were carried out with the Vienna *ab initio* simulation package (VASP), using the Perdew-Burke-Ernzerhof (PBE) exchange-correlation functional,[19] with dispersion interactions accounted for using Grimme's D2 method.[20] The combination of the PBE functional and the empirical D2 parameters lead to a PE unit cell of dimensions $a = 6.66$, $b = 4.56$, $c = 2.55$ Å,[21] in fairly good agreement with the experimentally measured values.[22] The D2 dispersion correction results in a negligible increase in computational cost.

A $1 \times 2 \times 9$ supercell of PE was created for the DFT calculations described in Secs. III A, III C, and III E, containing 72 CH_2 units distributed along four chains. A plane wave energy cut off of 520 eV was employed for these calculations, along with a Γ-centered Monkhorst-Pack k-point mesh ensuring approximately 20 special k-points per inverse Å along the reciprocal lattice vectors. For the DFT calculations employing the HSE06 exchange correlation functional[23,24] the plane wave energy cutoff was reduced to 400 eV, while the same set of k-points as for the PBE calculations were employed. Furthermore, due to the additional expense associated with the HSE06 functional, the structures described were not optimized with the functional; the energies were calculated for the structures arrived at from the optimizations carried out using the PBE-D2 functional. The dispersion interactions for the HSE06 calculations were described using the D2 approach, as described previously.

For the *ab initio* MD simulation described in Sec. III B, which was also carried out using the VASP package, a $1 \times 2 \times 9$ PE supercell was again used. The supercell employed was disproportionately extended along the (chain) c direction, in order to allow the individual chains to explore such extended conformational twists and distortions as may be associated with localized electron and hole states.[16,25] The plane wave energy cutoff for the MD simulation was reduced to 300 eV to allow access to relevant time scales within the available computer time. The k-point mesh employed was identical to that used for the structural optimizations. A MD time step of 0.5 fs was employed.

In the MD simulation, the PE was first equilibrated for 0.5 ps in the canonical ensemble, at $T = 10$ K, where a Nosè-Hoover thermostat[26,27] was used to enforce the constant temperature. Using the same approach, T was increased to 300 K over a period of 2.5 ps, and then held for 2.5 ps at 300 K. At this point in the simulation, the electron occupations were reset to reflect the $S = 1$ triplet exciton state (see Sec. III A), the electronic degrees of freedom quenched, and the simulation restarted in the microcanonical ensemble, with the electron occupations fixed, for a simulation time of 3 ps.

III. RESULTS AND DISCUSSION

A. Thermodynamics of C–H bond cleavage

To probe for the possibility and effect of C–H bond cleavage for PE in various electronic states, a single broken C–H bond was introduced into the PE supercell, by increasing the distance between a single pair of bonded C–H atoms to 2.5 Å—well beyond the typical C–H bond length of 1.1 Å. Structural optimizations were then carried out for the supercell, with fixed cell dimensions. The electron occupations were set at the beginning of each optimization, and held constant for its duration, for four distinct cases described below:

(i) All valence bands were doubly occupied; all included conduction bands were empty,
(ii) All valence bands were doubly occupied; of the included conduction bands, only the lowest contained a single electron (i.e., an additional electron is placed in the lowest conduction band),
(iii) All valence bands were doubly occupied except the highest, which was singly occupied; all included conduction

bands were empty (i.e., a hole is placed in the highest valence band),

(iv) A triplet exciton, i.e., the lowest energy exciton state, was introduced to the supercell; a spin-down electron was removed from the highest occupied band, while a spin-up electron was simultaneously introduced into the lowest unoccupied band, ensuring a total spin $S = 1$.

A triplet (singlet) exciton may be formed if an electron and a hole of like (unlike) spin become bound. AC-type high fields are expected to provide ample opportunity for the formation of excitons of both types. Guarded needle measurements indicate that for a 5 μm tip, at fields well below twice the space charge limited field, the charge density near the tip is of the order 10^3 C/m^3 and drops as r^{-1} away from the tip.[1] Such measurements for PE also indicate that the charge injection is symmetric with respect to polarity.[1] An AC waveform will therefore result in charge densities of order 10^3 C/m^3 passing through each other every half cycle, as the charge at the needle tip reverses. In PE under high AC-type fields the frequent meeting of opposite-polarity charge densities will cause electrons and holes of like and unlike spin to form triplet and singlet excitons, respectively.

Figure 1(a) shows schematically the energy levels associated with PE in the four electronic states. For cases (ii)–(iv) spin-polarized calculations were carried out. Using the approach described for case (iv), the system in the excitonic state can be legitimately modeled,[29] although a detailed description of the interactions between the electron and hole is lacking; such a description in general requires more sophisticated many-body techniques based on the *GW*-Bethe-Salpeter formalism.[30] The success of constrained semi-local DFT in reproducing the relaxations in the low-energy excited states of a conjugated polymer system, however,[31] suggests that this approach is sufficient for our purposes.

The results of the structural optimizations are summarized in Fig. 1(b). Cases (i)–(iii) yielded similar results: a re-formation of the broken C–H bond, and a final structure

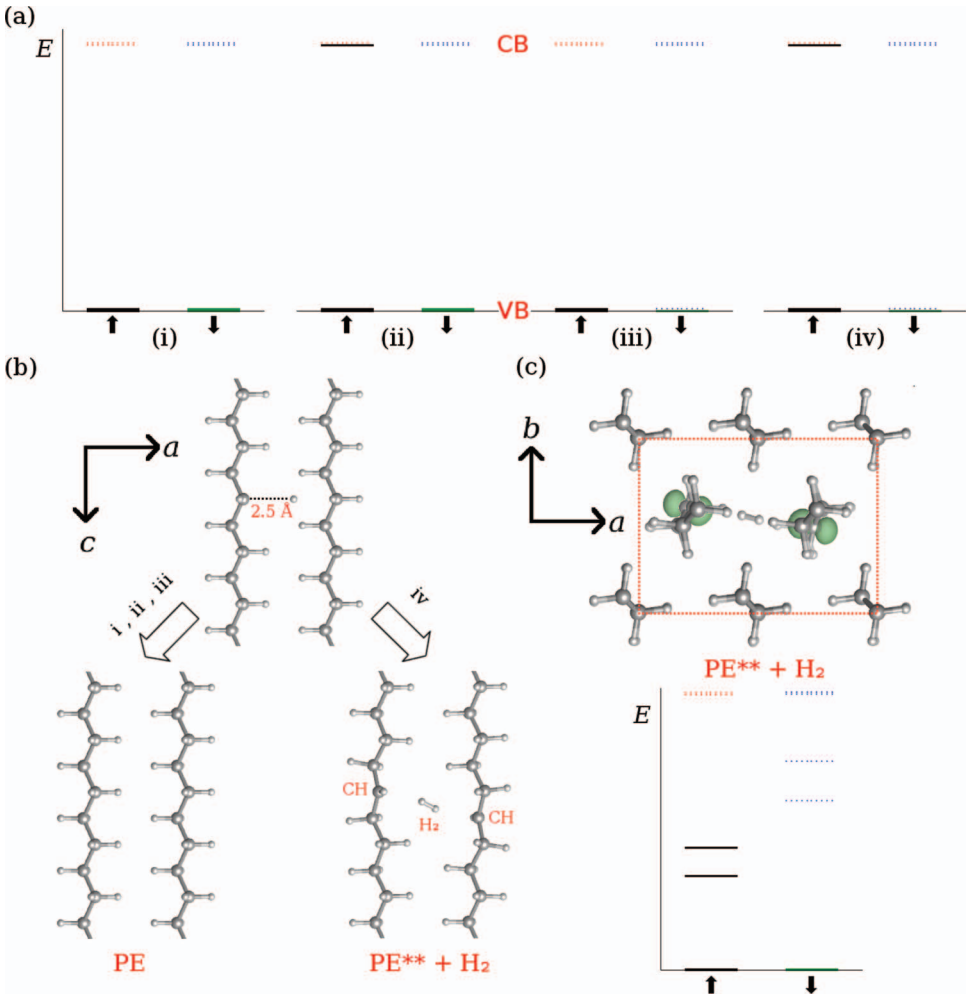

FIG. 1. (a) The energy levels at and between the valence band (VB) and conduction band (CB) edges are shown schematically for PE where the electron occupations correspond to optimizations (i), (ii), (iii), and (iv) described in the main text. Spin up (down) states correspond to the energy levels plotted on the left (right) in each case. Spin up (down) occupied states are indicated by full black (green) lines, while spin up (down) unoccupied states are indicated by dotted red (blue) lines. (b) Illustration of the results of the structural optimizations carried out with different electron occupations. For optimizations (i)–(iii) the broken C–H bond reformed, while for optimization (iv) the H atom abstracted a second H from the neighboring chain, forming H_2, and leaving one –CH– defect in each of the two adjacent main chains. Only two chains of the four in the unit cell are shown in each case. (c) The PE** + H_2 structure obtained from optimization (iv), viewed along the (chain) *c* direction. The magnetization density is plotted, with regions of positive magnetization density shown in green, and is tightly localized on the –CH– defects, confirming that these groups contain unpaired electrons, and should be considered as free radicals. The energy levels corresponding to the PE** + H_2 structure are shown. Illustrations created in part using the VESTA package.[28]

resembling PE. For case (iv), on the other hand, the lone H atom, during the course of the optimization, abstracted a second H atom from one of the –CH_2– units in a chain adjacent to that containing the first –CH– defect, forming an H_2 dimer. In the optimized structure, two neighboring chains each contained exactly one –CH– defect, and the H_2 dimer was present in the space in-between the two defect-containing chains (Fig. 1(c)). The energy of the resulting system, henceforth referred to as PE** + H_2, was compared to that of PE in the triplet state, hereafter referred to as PE (triplet),[32] and found to be lower by 2.4 eV, indicating that dissociation of PE (triplet) is thermodynamically strongly favored.

We note that a dissociative exciton recombination mechanism for PE was not identified in the non-spin-polarized DFT calculations described in Ref. 16, in which only the Γ-point was sampled. In an attempt to understand why dissociation was found to be a favorable mechanism in these calculations but was not identified as such in those described in Ref. 16, we repeated calculation (iv) with sampling of only the Γ-point and without spin-polarization (i.e., with the highest valence band and lowest conduction band both half-filled[16,17]). We did not find the result of this repeated calculation to be qualitatively different to that of the original calculation (iv), described above, so the origin of the differences with respect to the results of Ref. 16 remain unclear, although we note that there are several other differences (i.e., exchange-correlation functional employed, method of description of the electron-ion interactions, parameters used to describe the dispersion interactions, etc.) between the computational approach used for the calculations described here and for those of that paper.

A structural optimization was carried out for the PE** system alone (i.e., PE containing two –CH– defects). The ground state of this system was in the $S = 1$ state, with one unpaired electron on each of two –CH– defects, indicating that these are radicals. A plot of the magnetization density for PE** + H_2 (Fig. 1(c)) reveals that the unpaired electrons are tightly localized on the –CH– radicals, as expected. The interaction energy between the PE** and the H_2 in the PE** + H_2 system was 0.2 eV, where the energy of the H_2 dimer was taken as that of a vapor phase H_2 molecule, confirming an absence of chemical bonding between the two constituent parts. In dissociating from PE (triplet) (schematic energy levels shown in Fig. 1(a), case (iv)) to PE** + H_2 (energy levels shown in Fig. 1(c)) an occupied state and an unoccupied state (of opposite spin) would cross one another. This suggests a path for nonradiative exciton recombination in PE, via C–H bond scission, which provides a mechanism for the initiating step in high-field aging.

The difference in energy between the PE (triplet) and PE** + H_2 systems was also evaluated using the HSE06 functional, which includes 25% of the exact Hartree Fock exchange, and generally results in band gaps which are significantly closer to experimentally measured values. In that case the dissociated system was found to be 3.5 eV lower in energy than PE (triplet). The disparity of approximately 1.1 eV between the PBE and HSE06 energy differences mainly reflects the wider PE band gap associated with the HSE06 functional, which is larger than that associated with PBE by approximately 1.4 eV. In any case, the HSE06 calculations support the result that the dissociation of PE (triplet) is thermodynamically favorable.

B. *Ab Initio* MD simulation of exciton injection

Although the calculations just described indicate that dissociative recombination of excitons within PE is a possibility, other recombination mechanisms may present more likely alternatives. The exciton might become stabilized on a conformational distortion for long enough to recombine via radiative or other nondissociative routes. Chemical impurities, abundant in real PE (but not considered here), also offer a potential source of sites at which excitons can become trapped and recombine nondissociatively.[17] To investigate further the fate of excitons in pure PE, an *ab initio* MD simulation was performed, during which an exciton was injected into PE at temperature $T = 300$ K. We note that the MD results described here refer to a single representative simulation; other similar simulations were carried out and produced qualitatively similar results.

Figure 2(a) shows snapshots of the system taken during the simulation, after exciton injection ($t = 0$). Very soon after the injection ($t \sim 45$ fs), an H atom dissociated from the main chain, leaving a –CH– defect behind. Approximately 60 fs later, the dissociated H atom abstracted a second H atom from a neighboring chain, as was observed in structural optimization (iv) described above. After H abstraction and formation of the H_2 dimer, the resulting PE** + H_2 system did not undergo any qualitative structural changes for the remainder of the 3 ps simulation. Figure 2(c) shows a plot of the magnetization density of the system 121 fs after exciton injection, which indicates that the magnetization in the dissociated system is strongly localized on the CH· radicals, as expected.

The evolution of the Kohn-Sham eigenvalues corresponding to the conduction and valence band edges is plotted in Fig. 2(b), for -250 fs $< t <$ 250 fs. The energy is referenced to that of the highest occupied eigenvalue for PE at $T = 0$. Prior to exciton injection, the occupied state fluctuates around a value approximately 0.2 eV above this value. Very soon after injection (after approximately 30 fs), the filled conduction level begins to drop in energy rapidly, while the empty valence level simultaneously increases. The levels meet and cross 48 fs after injection, just as the C–H bond is breaking. For the next 90 fs the eigenvalues fluctuate somewhat violently, as the unbonded H atom moves around among the chains. Approximately 120 fs after injection, the fluctuations become smaller, just as the first H atom abstracts the second H atom. For the rest of the 3 ps simulation, the levels fluctuate around values close to those shown for the PE** + H_2 system in Fig. 1(c), as the PE has fully dissociated into PE** and H_2.

The rapid dissociation of PE (occurring after only a few tens of fs) after exciton injection in the MD simulation suggests that exciton recombination could be responsible for C–H bond scission and radical formation in pure PE at room temperature, and suggests a low energetic barrier to the dissociation. In order to make a quantitative estimate of the barrier to radical formation, we employed CINEB calculations, described in Sec. III C.

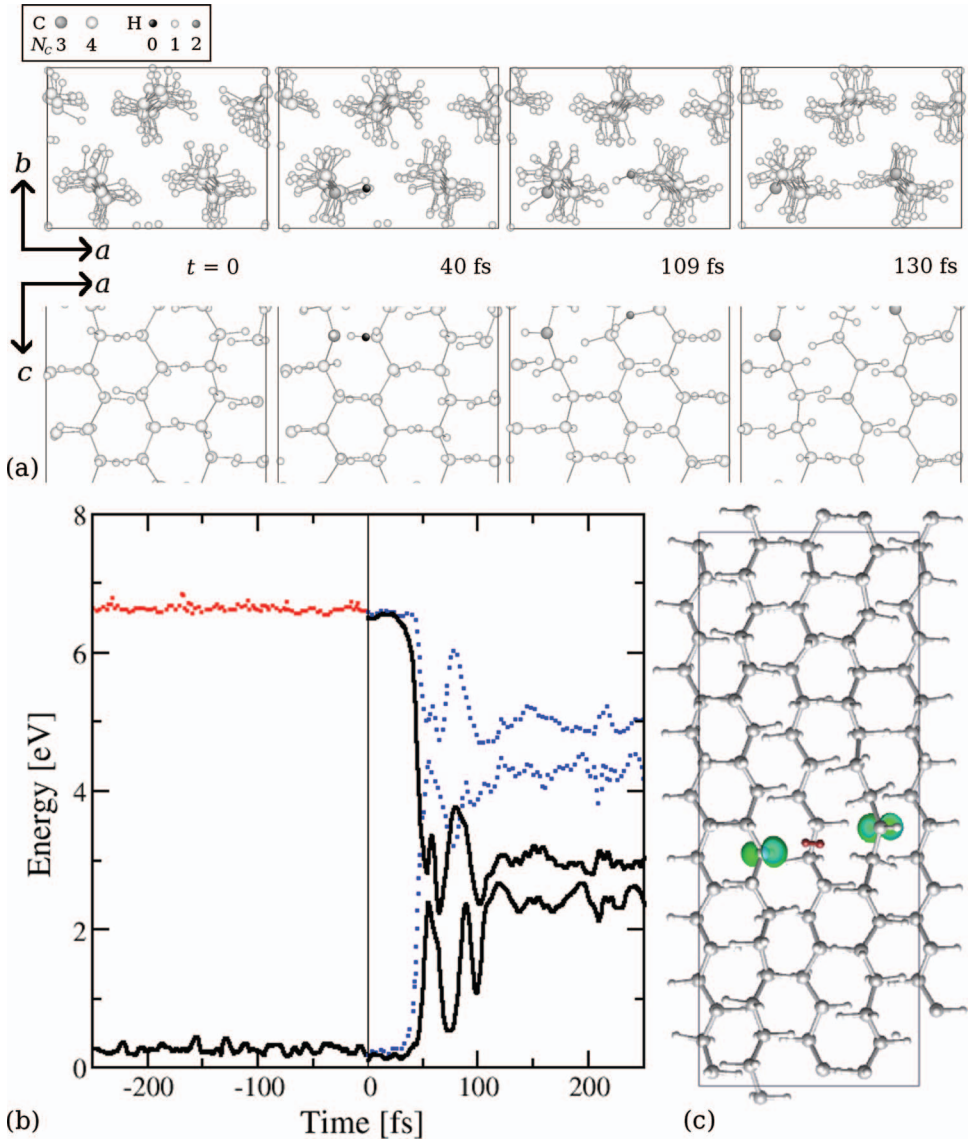

FIG. 2. (a) Snapshots taken at time t during the *ab initio* MD simulation of PE, where $t = 0$ refers to the point at which the exciton was injected. Atoms are shaded according to coordination number N_C. The snapshots illustrate C–H bond scission and the subsequent H abstraction. (b) Evolution of the highest occupied and lowest unoccupied energy eigenvalues of the system for 250 fs prior to ($t < 0$) and after ($t > 0$) exciton injection. The zero of energy is the value of the highest occupied PE eigenvalue at $T = 0$. The colors of the energy levels correspond to those in Fig. 1(a). Prior to exciton injection, each of the two levels shown is doubly occupied (the colors shown correspond to spin up states). Upon triplet exciton injection, both hitherto spin-degenerate states split into an occupied spin up (full black lines) and an unoccupied spin down (dotted blue lines) state. (c) Magnetization density plot of the system at $t = 121$ fs. The magnetization is tightly localized on the –CH– groups along the main chains, indicating that these groups have unpaired electrons. The H_2 dimer is shown in deep red for clarity. Illustrations created in part using the AtomEye package.[33]

C. Energetic barriers to radical formation

The height of the energetic barrier to bond scission was estimated using CINEB DFT calculations, which provides a method to identify saddle points and minimum energy paths between known metastable endpoints.[18] The initial end-points used for the calculations were the intact PE (triplet) structure, and the PE** + H_2 structure. The electron occupations were set as in structural optimization (iv), such that the first image represents PE in the triplet exciton state, and the last image represents the PE** + H_2 system in the $S = 1$ state.

It was found that the PE (triplet) system can lower its energy through a distortion of the PE chains, the exciton states becoming localized on the distorted region. The transition from PE (triplet) to the distorted structure (henceforth referred to as PE (localized)) is barrierless (Fig. 3(b)), and leads to an overall reduction in energy of the system of approximately 30 meV. The PE (localized) system was hence used as an intermediate image in the CINEB calculations, which proceeded as PE (triplet) → PE (localized) → PE** + H_2; the corresponding CINEB estimated minimum energy path is shown by the blue circles and black circles in Fig. 3(b).

The PE (localized) structure (Fig. 3(a)) is characterized by a deviation of the C–C–C–C torsional angles with respect to the all-*trans* PE value of 180°, by up to ±5°, as well as a lengthening of the C–H bond lengths of up to 20 mÅ. This twisting of the PE chains is restricted to a region approximately seven C_2H_4 units in length, with the maximal deviation in torsional angle occurring at the center (i.e., with respect to the chain direction) of the distortion; the 180° *trans*

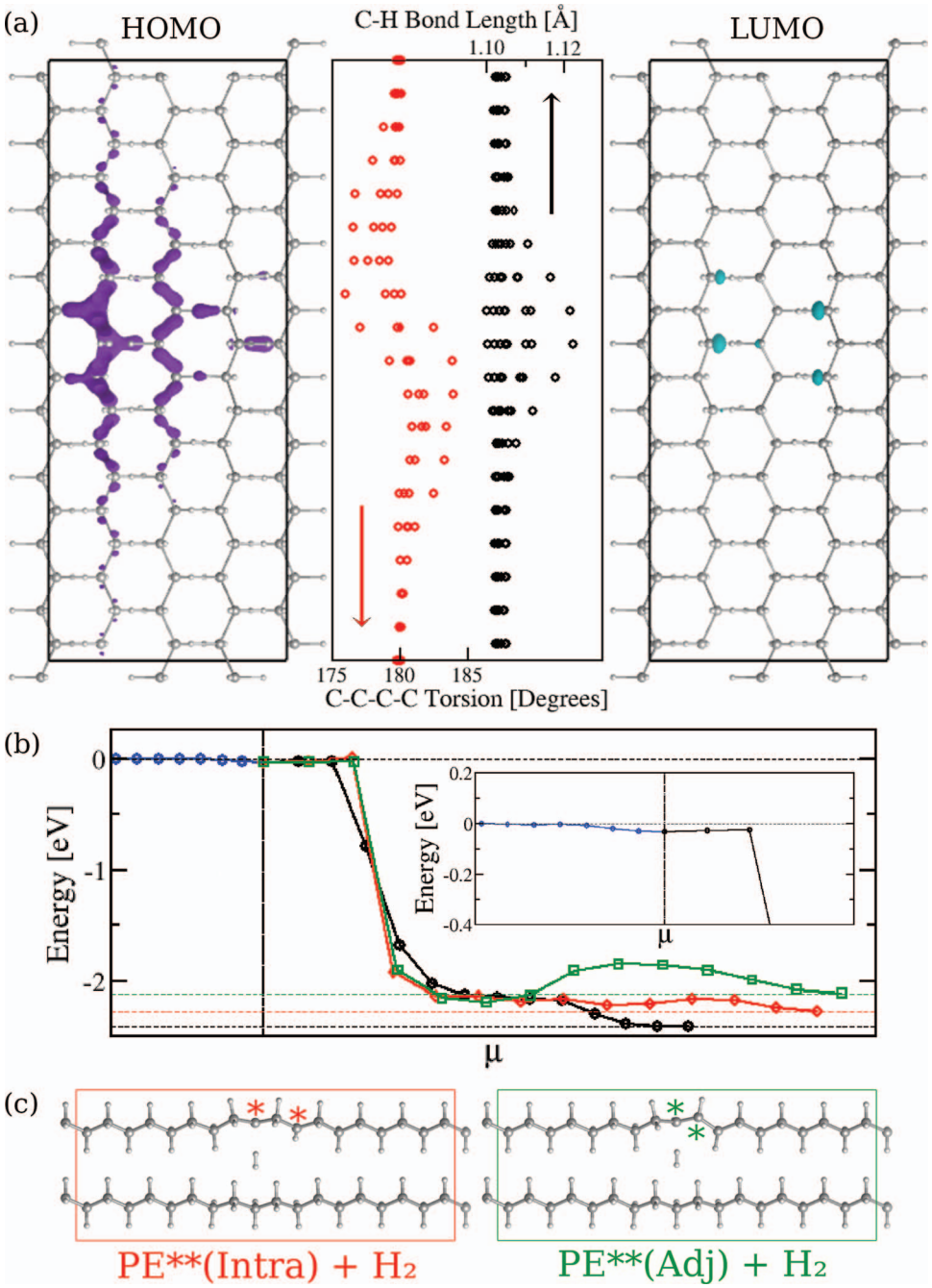

FIG. 3. (a) The partial charge density associated with the HOMO and LUMO states, which are both half-filled, are plotted for the PE (localized) system. C–H bond lengths and C–C–C–C torsional angles are plotted for the four chains for the PE (localized) system, revealing a twist in the chains as well as a lengthening of the C–H bonds in the region on which the exciton states are localized. (b) Minimum energy paths between the PE (triplet) system and the dissociated PE** + H_2 (black circles), PE**(Intra) + H_2 (red diamonds), and PE**(Adj) + H_2 (green squares) systems, calculated using the CINEB method, are plotted versus the reaction coordinate μ. All paths take place through the PE (localized) system, whose energy is approximately 30 meV lower than that of PE (triplet). The PE (triplet) → PE (localized) path is indicated by the blue circles; the vertical black line indicates the shallow energy minimum associated with the distorted structure. The inset shows a close-up of this region. (c) The PE**(Intra) + H_2 and the PE**(Adj) + H_2 structures. The position of the –CH– groups along the chains are indicated by the asterisks in each case. Only two of the four chains in the cell are shown for clarity.

value is recovered for regions of the chains furthest away from the distortion. Likewise, the C–H bond lengthening is restricted to a region approximately four C_2H_4 units in length and is most pronounced at the center of the distorted region.

The highest occupied molecular orbital (HOMO) and lowest unoccupied molecular orbital (LUMO) are both strongly localized on the four C–H bonds for which the bond lengthening is greatest, which suggests a weakening of these bonds; the half-filled LUMO and HOMO states represent the filling of an anti-bonding orbital and the emptying of a bonding orbital, respectively. However, the PE (localized) system remains stable with respect to C–H bond breaking; the CINEB calculations suggest that despite the bond-weakening, a barrier remains to the breaking of the C–H bonds on which the exciton is localized, albeit much smaller than the $\gtrsim$4 eV normally associated with C–H bonds. The barrier to C–H bond

scission from the PE (localized) structure is indeed very small, estimated at 25 meV, a result which is consistent with the observation of bond breaking in the MD simulation a few tens of fs after exciton injection.

After the initial C–H bond scission, no barrier was associated with the abstraction of the second H from a neighboring chain and the formation of the PE** + H_2 structure (Fig. 3(b), black circles), which is consistent with structural optimization (iv). In order to explore the importance of the proximity of the –CH·– radicals in the dissociated structure, CINEB calculations were carried out with alternative endpoints, in which the radicals were positioned along the same PE chain, as described in Sec. III D.

D. Proximity of the CH· radicals

In the structural optimization, as well as in the *ab initio* MD simulation and the CINEB calculation described in Sec. III C, the C–H bond scission and subsequent H abstraction took place via neighboring chains, meaning that the –CH– radicals produced were separated by a distance approximately equal to the inter-chain separation. Here we are interested in the possibility of the creation of radicals which lie on the same PE chain, which is likely to involve an energetic barrier to abstraction. This was investigated by two further CINEB calculations, in which the PE** + H_2 end point was replaced by a similar system in which the second CH· radical is on the same chain as the first. Two such possibilities were considered, which are illustrated in Fig. 3(c): in the first case (referred to as PE(Intra)** + H_2) a single $–CH_2–$ unit separates the radicals, and in the second case (PE(Adj)** + H_2), the radicals are directly adjacent. For the latter case, the torsional H–C–C–H angle associated with the two CH· radicals was 86° (i.e., distorted by ∼90° with respect to the *trans* H–C=C–H conformation associated with the ground state vinyl defect in PE), and the C–C bond length was 1.46 Å. Such a conformation is reminiscent of the equilibrium geometry of the lowest excited $^3A_1$ triplet state of the ethylene molecule,[34,35] and agrees well with the (spin-unpolarized) DFT optimized values for an exciton trapped at a vinyl defect reported by Ceresoli and co-workers, of 84° and 1.45 Å.[17]

The optimized structures of the PE(Intra)** + H_2 and PE(Adj)** + H_2 systems were higher in energy than the original PE** + H_2 system (i.e., in which the radicals are on neighboring chains) by 0.13 eV and 0.30 eV, respectively. The calculated minimum energy paths between PE (localized) and these structures are shown in Fig. 3(a) by the red diamonds and green squares, respectively. The barrier associated with the initial C–H scission is similar in all cases, although the minimum energy paths to the PE(Intra)** + H_2 and PE(Adj)** + H_2 structures include a second barrier, associated with the abstraction of the second H atom, estimated at 60 meV and 340 meV, respectively. The increased energy of the PE(Intra)** + H_2 and PE(Adj)** + H_2 systems with respect to the PE** + H_2 system, and the higher barriers associated with their formation, can be understood in terms of Pauli repulsion and the greater proximity of the like-spin electrons associated with the radicals when abstraction takes place from the same chain as C–H bond scission.

The energetic barrier of 340 meV possibly precludes the dissociation of PE (triplet) into the PE(Adj)** + H_2 system. A system in which CH· radicals are directly adjacent on the same chain may be attained, however, if an exciton localizes on a pre-existing vinyl defect.[17] In principle, a triplet exciton trapped at such an adjacent pair of CH· radicals, with a H–C–C–H torsional angle of 180° as for the ground state vinyl defect (referred to here as $PE(Adj)^{**}_{trans}$), may relax back to the $S = 0$ PE (vinyl) ground state via phosphorescence and the formation of a HC=CH double bond. A nonradiative, nondissociative, recombination pathway is also available, to a $S = 1$ excited state (referred to here as $PE(Adj)^{**}_{dist}$) via a structural distortion, characterized by a ∼90° twist in the H–C–C–H dihedral and a reduction in the distance between the two C atoms, as the π bond between them is broken.[17] The final conformation resulting from this distortion resembles the excited state of the ethylene molecule, as has been noted previously.[17] Schematic energy level diagrams shown in Fig. 4(a) illustrate the nonradiative recombination pathway between the triplet exciton $PE(Adj)^{**}_{trans}$ system and the $S = 1$ $PE(Adj)^{**}_{dist}$ distorted system, as well as the radiative pathway between $PE(Adj)^{**}_{trans}$ and the $S = 0$ PE (vinyl) ground state.

E. The possibility of radiative recombination

In order to understand more fully the exciton recombination pathways for the PE(Adj)** system, an *ab initio* MD simulation was carried out, in which a triplet exciton was injected into a 216-atom cell containing four chains of PE including one vinyl defect and an H_2 dimer (included in the simulation to probe the possibility of H_2 dissociation and C–H re-formation). The energy cutoff, equilibration procedure, supercell size, etc., were the same as for the MD simulation described earlier.

Figure 4 shows the evolution of the Kohn-Sham energy eigenvalues and the H–C–C–H torsional angle for $-500\ \text{fs} < t < 3000\ \text{fs}$, where $t = 0$ is the point at which the exciton was injected. Immediately upon injection, the value about which the torsional angle fluctuated changed from ∼180° to ∼270°, and the occupied spin-up conduction and unoccupied spin-down valence Kohn-Sham levels crossed each other, indicating (nonradiative and nondissociative) exciton recombination, as the $PE(Adj)^{**}_{trans}$ system transitioned to $PE(Adj)^{**}_{dist}$. Interestingly, however, we see the Kohn-Sham levels re-cross at several points during the simulation (indicated by the vertical red lines), accompanied by simultaneous large deviations in the torsional angle from 270°. For the periods during which the levels have re-crossed, a radiative transition to the $S = 0$ PE (vinyl) system is possible. We surmise that radiative recombination will likely occur for an exciton trapped at adjacent CH· radicals in PE, although after a relatively long time, since the amount of time for which radiative recombination is possible (i.e., during those periods when the levels have re-crossed) is small relative to the amount of time when it is not.

An estimate of the energy of the photon released upon the relaxation of the $PE(Adj)^{**}_{trans}$ ($S = 1$) system to

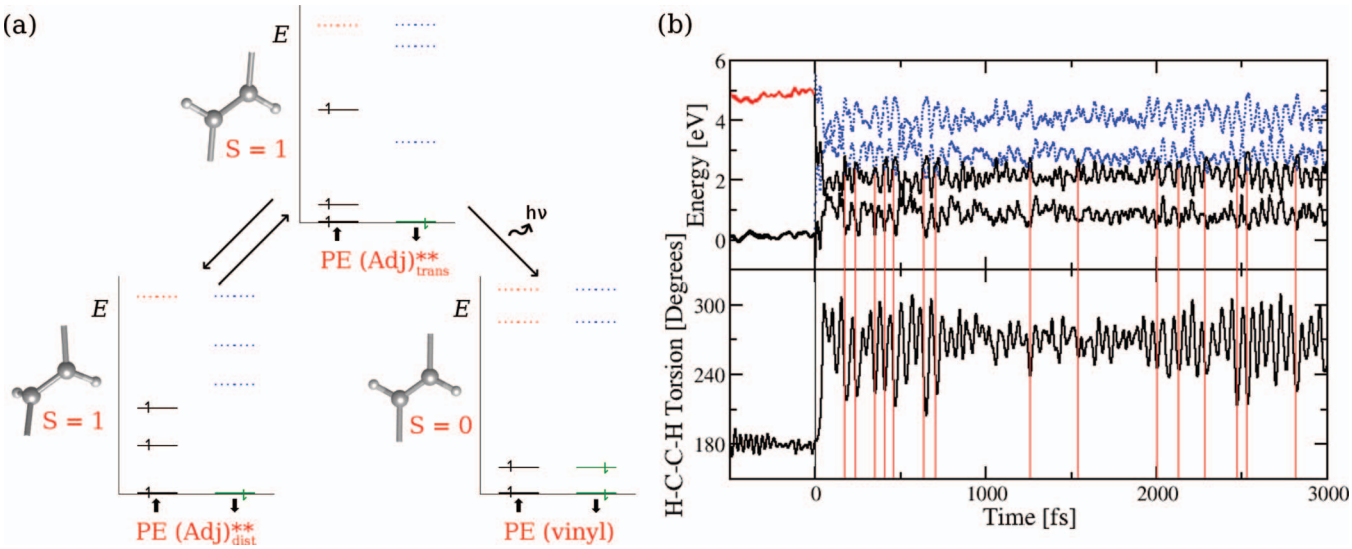

FIG. 4. (a) Energy levels are shown schematically for PE containing two adjacent CH· radicals, in the *trans* H–C–C–H torsional conformation (PE(Adj)$^{**}_{trans}$), and in the ∼90° distorted conformation (PE(Adj)$^{**}_{dist}$), as well as for PE containing a vinyl defect (PE (vinyl)). (b) Evolution of the highest occupied and lowest unoccupied Kohn-Sham energy levels (colors as for Fig. 2) and the H–C–C–H torsional angle for the PE (vinyl) + H_2 system. The zero of energy is the value of the highest occupied eigenvalue of the PE (vinyl) + H_2 system at T = 0. A triplet exciton is injected into the system at $t = 0$. Upon exciton injection, the 180° *trans* H–C–C–H torsional angle immediately increases by ∼90°, while the occupied spin-up level in the conduction band and the unoccupied spin-down level in the valence band cross, heralding a recombination and transition to the PE(Adj)$^{**}_{dist}$ system. Brief level re-crossings occur at several subsequent times during the 3 ps simulation, concurrent with large fluctuations in the H–C–C–H torsional angle (indicated by the vertical red lines), allowing for the possibility of radiative recombination and transition to the PE (vinyl) structure.

the $S = 0$ PE (vinyl) system via phosphorescence was taken as E[PE(Adj)$^{**}_{trans}$] − E[PE (vinyl)] = 3.10 eV, where E[PE(Adj)$^{**}_{trans}$] denotes the energy of the PE(Adj)$^{**}_{trans}$ system (in the $S = 1$ state), and E[PE (vinyl)] denotes the energy of the PE (vinyl) system (in the $S = 0$ state). This calculation constitutes only a rough estimate of the photon energy, given the level of theory used in the calculation (neglecting a detailed description of the electron-hole interactions), and the fact that the photon emission in reality does not correspond to a transition between the vibrational ground states of the relevant systems. Indeed, our MD simulation would suggest that the eventual radiative recombination is likely to take place from a PE(Adj)$^{**}_{trans}$ system which is relatively far from the vibrational ground state, as a consequence of the alternative nonradiative transition path to PE(Adj)$^{**}_{dist}$. Nevertheless, our predicted photon energy corresponds to a wavelength of 400 nm, which is reasonably consistent with phosphorescence measurements for low density PE, which show three pronounced peaks at around 429, 445, and 459 nm.[36] Repeating this calculation with the HSE06 functional a photon wavelength of 412 nm is estimated, in slightly closer agreement with the experimental measurements. We surmise that radiative recombination at adjacent CH· radicals to form ethylenic vinyl defects may be responsible for a peak in the phosphorescence spectra of polyethylene, although more detailed calculations and possibly further experiments are needed to make this link conclusively.

IV. SUMMARY AND CONCLUSIONS

In summary, our *ab initio* MD simulations and density functional calculations have suggested a microscopic route by which high-field aging may occur in pure PE, via the creation of CH· radical groups, through the dissociative recombination of excitons. Here we give a brief summation of each of the main conclusions arrived at from this work:

1. C–H bond cleavage is thermodynamically favored in pure PE upon injection of a triplet exciton; cleavage is not favored upon the injection of a conduction-band electron or a valence-band hole.
2. The resulting bond cleavage occurs very rapidly upon exciton injection; the exciton does not become trapped at a long-lived structural distortion of the PE. Considering the very small (10^{-6}) quantum efficiency of PE,[4] the small barrier to C–H dissociation (∼25 meV) found in our CINEB calculations and the corresponding short time for dissociation to take place upon exciton injection (∼50 fs) observed in our MD simulations, the dissociative mechanism presented here represents a candidate for the dominant exciton recombination pathway in PE.
3. The damage caused to PE resulting from bond cleavage owing to exciton recombination is expected to scale with the number of exciton recombinations per unit time. This is consistent with the experimentally observed increase in the degree of aging with the applied field strength, or with the amount of time exposed to the field, either of which can in general be expected to lead to a greater number of recombination events.
4. The exciton can create and localize on a metastable structural distortion, characterized by a twist in the C–C–C–C torsional angle and a lengthening of the C–H bond lengths within the distorted region. However, the energetic barrier to C–H bond cleavage from the distorted structure is comparable to the thermal energy at

room temperature, so the distorted structure will be extremely short-lived and cleavage will occur rapidly.

5. Upon C–H bond cleavage, H abstraction is likely to take place via a neighboring PE chain, as this process is energetically barrierless. H abstraction from the same chain in which the first cleavage event occurred is associated with a significant energetic barrier, owing to the Pauli repulsion.
6. An exciton trapped at a pair of adjacent –(CH)– radicals may recombine radiatively to form a vinyl defect. However, this path is hindered by the existence of the nonradiative path identified by Ceresoli *et al.* Radiative recombination is therefore predicted to take place on a significantly protracted time scale.

ACKNOWLEDGMENTS

The authors would like to thank Steven Boggs for numerous insightful discussions. This work was supported by a Multi-University Research Initiative (MURI) grant from the Office of Naval Research (ONR). This research was supported in part by the National Science Foundation (NSF) through XSEDE resources provided by the Texas Advanced Computing Center under Grant No. TG-DMR080058N.

[1]S. A. Boggs, IEEE Trans. Dielectr. Electr. Insul. **12**, 929 (2005).
[2]L. A. Dissado and J. C. Fothergill, *Electrical Degradation and Breakdown in Polymers* (IET, London, 1992).
[3]C. Laurent, in *Proceedings of the 1998 IEEE 6th International Conference on Conduction and Breakdown in Solid Dielectrics* (IEEE, Västerås, 1998), pp. 1–12.
[4]S. Le Roy, G. Teyssedre, and C. Laurent, IEEE Trans. Dielectr. Electr. Insul. **12**, 644 (2005).
[5]Y. Cao and S. A. Boggs, IEEE Trans. Dielectr. Electr. Insul. **12**, 690 (2005).
[6]S. Bamji, A. Bulinski, and M. Abou-Dakka, IEEE Trans. Dielectr. Electr. Insul. **16**, 1376 (2009).
[7]D. K. Davies, J. Phys. D: Appl. Phys. **5**, 162 (1972).
[8]A. Huzayyin, S. A. Boggs, and R. Ramprasad, IEEE Trans. Dielectr. Electr. Insul. **17**, 920 (2010).
[9]A. Huzayyin, S. A. Boggs, and R. Ramprasad, IEEE Trans. Dielectr. Electr. Insul. **17**, 926 (2010).
[10]T. Miyashita, IEEE Trans. Electr. Insul. **EI-6**, 129 (1971).
[11]C. Mayoux, IEEE Trans. Electr. Insul. **EI-11**, 139 (1976).
[12]F. Gugumus, Polym. Degrad. Stab. **76**, 329 (2002).
[13]A. Ariffin, P. Lewin, and S. Dodd, IEEE Trans. Dielectr. Electr. Insul. **18**, 130 (2011).
[14]B. Montanari and R. Jones, Chem. Phys. Lett. **272**, 347 (1997).
[15]S. Serra, E. Tosatti, S. Iarlori, S. Scandolo, and G. Santoro, Phys. Rev. B **62**, 4389 (2000).
[16]D. Ceresoli, M. C. Righi, E. Tosatti, S. Scandolo, G. Santoro, and S. Serra, J. Phys.: Condens. Matter **17**, 4621 (2005).
[17]D. Ceresoli, E. Tosatti, S. Scandolo, G. Santoro, and S. Serra, J. Chem. Phys. **121**, 6478 (2004).
[18]G. Henkelman, B. P. Uberuaga, and H. Jónsson, J. Chem. Phys. **113**, 9901 (2000).
[19]J. P. Perdew, K. Burke, and M. Ernzerhof, Phys. Rev. Lett. **77**, 3865 (1996).
[20]S. Grimme, J. Comput. Chem. **27**, 1787 (2006).
[21]C.-S. Liu, G. Pilania, C. Wang, and R. Ramprasad, J. Phys. Chem. A **116**, 9347 (2012).
[22]G. Avitabile, R. Napolitano, B. Pirozzi, K. D. Rouse, M. W. Thomas, and B. T. M. Willis, J. Polym. Sci.: Polym. Lett. Ed. **13**, 351 (1975).
[23]J. Heyd, G. E. Scuseria, and M. Ernzerhof, J. Chem. Phys. **118**, 8207 (2003).
[24]J. Paier, M. Marsman, K. Hummer, G. Kresse, I. C. Gerber, and J. G. Ángyán, J. Chem. Phys. **124**, 154709 (2006).
[25]S. Serra, S. Iarlori, E. Tosatti, S. Scandolo, M. Righi, and G. Santoro, Chem. Phys. Lett. **360**, 487 (2002).
[26]S. Nosé, J. Chem. Phys. **81**, 511 (1984).
[27]W. G. Hoover, Phys. Rev. A **31**, 1695 (1985).
[28]K. Momma and F. Izumi, J. Appl. Crystallogr. **41**, 653 (2008).
[29]M. Bernasconi, G. L. Chiarotti, P. Focher, M. Parrinello, and E. Tosatti, Phys. Rev. Lett. **78**, 2008 (1997).
[30]S. Ismail-Beigi and S. G. Louie, Phys. Rev. Lett. **90**, 076401 (2003).
[31]E. Artacho, M. Rohlfing, M. Côté, P. D. Haynes, R. J. Needs, and C. Molteni, Phys. Rev. Lett. **93**, 116401 (2004).
[32]The hole and electron states are delocalized in this system. The system may lower its energy by a few tens of meV by localization of the exciton on a structural distortion, as discussed in Sec. III C.
[33]J. Li, Model. Simul. Mater. Sci. Eng. **11**, 173 (2003).
[34]F. Qi, O. Sorkhabi, and A. G. Suits, J. Chem. Phys. **112**, 10707 (2000).
[35]M. Barborini, S. Sorella, and L. Guidoni, J. Chem. Theory Comput. **8**, 1260 (2012).
[36]C. Laurent, F. Massines, C. Mayoux, D. Ryder, and C. Olliff, in *IEEE Conference on Electrical Insulation and Dielectric Phenomena (CEIDP), Virginia Beach, USA* (IEEE, 1995), pp. 93–96.